Mills, G. A., E. R. Boedeker, and A. G. Oblad, "Chemical Characterization of Catalysts. I. Poisoning of Cracking Catalysts by Nitrogen Compounds and Potassium Ion," *J. Am. Chem. Soc.*, **72**, 1554 (1950).

Nace, D. M., S. E. Voltz, and V. W. Weekman, Jr., "Application of a Kinetic Model for Catalytic Cracking-Effects of Charge Stocks," *Ind. Eng. Chem. Process Design Develop.*, **10**, 530 (1971).

Oblad, A. G., T. H. Milliken, Jr., and G. A. Mills, "Chemical Characteristics and Structure of Cracking Catalysts," *Advances in Catalysis*, Academic Press, New York and London, vol. III, p. 199 (1951).

Ozawa, Y., "The Structure of a Lumpable Monomolecular System for Reversible Chemical Reactions," *Ind. Eng. Chem. Fundamentals*, **12**, 191 (1973).

———, and K. B. Bischoff, "Coke Formation Kinetics on Silica-Alumina Catalyst," *Ind. Eng. Chem. Process Design Develop.*, **7**, 22 (1968).

Paraskos, J. A., Y. A. Shah, J. D. McKinney, and N. L. Carr, "A Kinematic Model for Catalytic Cracking in a Transfer Line Reactor," *ibid.*, **15**, 165 (1976).

Plank, C. J., and D. M. Nace, "Coke Formation and Its Relationship to Cumene Cracking," *Ind. Eng. Chem.*, **47**, 2374 (1955).

Prasad, K. B. S., and L. K. Doraiswamy, "Effect of Fouling in a Fixed-Bed Reactor for a Complex Reaction: Test of Proposed Model and Formulation of an Optimal Policy," *J. Catal.*, **32**, 384 (1974).

Prater, C. D., and R. M. Lago, "Kinetics of the Cracking of Cumene by SiO_2-Al_2O_3 Catalysts," *Advances in Catalysis*, vol. VIII, p. 238 (1956).

Reif, H. E., R. F. Kress, and J. S. Smith, "How Feeds Affect Cat Cracker Yields," *Petrol. Refiner*, **40**, No. 5, 237 (1961).

Rudershausen, C. G., and C. C. Watson, "Variables Affecting Activity of Molybdena-Alumina Hydroforming Catalyst in Aromatization of Cyclohexane," *Chem. Eng. Sci.*, 3, 110 (1954).

Sachanen, A. N., *The Chemical Constituents of Petroleum*, pp. 289-296, 303, Reinhold, New York (1945).

Sadana, A., and L. K. Doraiswamy, "Effect of Catalyst Fouling in Fixed-, Moving-, and Fluid-Bed Reactors," *J. Catal.*, **23**, 147 (1971).

Shneider, G. S., I. I. Mukhin, M. A. Chueva, and Yu. S. Kogan, "A Kinematic Assessment of the Effect of the Fractional and Chemical Composition of the Crude on Catalytic Cracking Rate in a Fluidized Bed," *Chem. Tech. Fuels Oils (USSR)*, **1,2**, 13 (Jan.-Feb., 1969 (English translation).

Service, W. J., Jr., "Characterization and Preparation of Catalytic Feed Stocks," *Petrol. Chem. Eng.*, **32**, No. 12, C-31-C-36 (Nov., 1960).

Shankland, R. V., "Industrial Catalytic Cracking," *Advances in Catalysis*, Academic Press, New York and London, vol. VI, p. 271 (1954).

Szépe, S., and O. Levenspiel, "Catalyst Deactivation," Chemical Reaction Engineering, Proceedings of Fourth European Symp., Brussels 1968, 265, Pergamon Press, Oxford (1971).

Van Nes, K., and H. A. Van Westen, *Aspects of the Constitution of Mineral Oils*," pp. 335-347, Elsevier, New York (1951).

Voltz, S. E., D. M. Nace, and V. W. Weekman, Jr., "Application of a Kinetic Model for Catalytic Cracking—Some Correlations of Rate Constants," *Ind. Eng. Chem. Process Design Develop.*, **10**, 538 (1971).

Voltz, S. E., D. M. Nace, S. M. Jacob, and V. W. Weekman, Jr., "Application of a Kinetic Model for Catalytic Cracking—III. Some Effects of Nitrogen Poisoning and Recycle," *ibid.*, **11**, 261 (1972).

Voorhies, A., "Carbon Formation in Catalytic Cracking," *Ind. Eng. Chem.*, **37**, 318 (1945).

Weekman, V. W., Jr., "A Model of Catalytic Cracking Conversion in Fixed, Moving, and Fluid-Bed Reactors," *Ind. Eng. Chem. Process Design Develop.*, **7**, 90 (1968).

———, and D. M. Nace, "Kinetics of Catalytic Cracking Selectivity in Fixed, Moving, and Fluid Bed Reactors," *AIChE J.*, **16**, 397 (1970).

Wei, J., and J. C. W. Kuo, "A Lumping Analysis in Monomolecular Reaction Systems," *Ind. Eng. Chem. Fundamentals*, **8**, No. 1, 114 (1969).

White, P. J., "How Cracker Feed Influences Yield," *Hydrocarbon Process Petrol. Refiner*, **47**, No. 5, 103 (1968).

———, "How Cracker Feed Influences Yield," *Preprint No. 24-68*, API Division of Refining, 33rd Mid-Year Meeting, Philadelphia, Pa. (May, 1968).

Wojciechowski, B. W., "A Theoretical Treatment of Catalyst Decay," *Can. J. Chem. Eng.*, **46**, 48 (1968).

———, J. A. Juusola, and J. Downie, "A Phenomenological Classification of Catalyst Behavior," *Can. J. Chem. Eng.*, **47**, 338 (1969).

Wollaston, E. G., W. J. Haflin, W. D. Ford, and G. J. D'Souza, "FCC Model Valuable Operating Tool," *Oil Gas J.*, **87**, (Sept. 22, 1975).

Manuscript received December 1, 1975; revision revised March 18 and accepted April 5, 1976.

Basic Concepts of Spray Dryer Design

The major parameters in the design of spray dryers are discussed. A Lagrangian approach, combining experimental data with theoretical concepts, is proposed to develop design methods. Vortex flow patterns, obtained experimentally in a laboratory size chamber, are correlated and presented.

Based on this design methodology, computational methods are given to calculate droplet trajectories and hence to predict the optimum chamber dimensions and operating conditions for maximum thermal efficiency and/or minimum operating cost. Application of these basic principles is illustrated by the design of an industrial size, spray drying chamber for a specific feed solution and production rate.

W. H. GAUVIN
and
S. KATTA

Department of Chemical Engineering
McGill University
Montreal, Quebec

SCOPE

The growing importance of spray drying is abundantly evident from the ever increasing number of industrial applications in the production of pharmaceuticals, detergents, food products, pigments, ceramics, and a large number of organic and inorganic chemical compounds. In spite of these impressive developments and of the large number of fragmented experimental studies which have appeared in the technical literature during the past three decades, the design of spray dryers has remained largely empirical; it is still mainly based on the extensive experience and the vast body of operating data which the manufacturers have acquired over the years.

S. Katta is with Westinghouse Research Laboratories, Pittsburgh, Pennsylvania.

The objective of the present work was to develop a basis for spray dryer design by combining fundamental principles of fluid mechanics and transport phenomena with experimental evidence originating from both the studies carried out in this laboratory and from those published in the literature.

A specific chamber geometry (with a cylindrical upper part where the drying gas is admitted tangentially, and with a 55 deg. conical bottom) was chosen for illustrative purposes, since detailed flow patterns were known in this case and since this type is commonly employed in industry. The analysis can definitely be extended to other geometries provided the flow patterns are known. In the present case, detailed tangential and axial velocity profiles measured in a laboratory spray dryer of the same geometry were used in the computations.

In earlier studies (Gauvin et al. 1975; Katta and Gauvin, 1975), droplet trajectories for both sprays of water and of calcium lignosulfonate solutions in three-dimensional motion in the same chamber, as was used in the present investigation, were predicted in good agreement with the experimental results. The effects of a number of operating variables on the capacity and the efficiency of the spray dryer were also experimentally studied. In a further paper, the behavior of sprays in the near vicinity of a pneumatic atomizer was investigated both experimentally and theoretically by Katta and Gauvin (1975), and the evaporation rate in this zone was found to be negligible.

In the present work, the major design parameters are identified as the physical properties and drying characteristics of the feed solution; the droplet size distribution (DSD) and the largest droplet diameter; the type of atomizer and the drying gas flow patterns, both of which influence the motion of droplets in the spray drying chamber; and the heat and mass transfer rates in the constant and falling rate periods.

Based on these parameters, a computer aided theory of spray dryer design is elaborated, which is then applied, for illustrative purposes, to the design of a spray drying chamber of industrial size capable of drying a 30% sodium nitrate solution at the production rate of 1 000 kg/h of solids, employing a single pressure atomizing nozzle. The design was based on the criterion that the dimensions of the chamber shall be such that the largest droplet in the initial spray shall be dry (or, more exactly, shall reach the specified residual moisture content) before it reaches the chamber wall. From a practical point of view, this criterion is admittedly overconservative but can be relaxed as experience is gained with the use of this model.

CONCLUSIONS AND SIGNIFICANCE

The theoretical and experimental considerations presented in this study appear to have established a logical basis for the design of spray dryers. From a knowledge of the drop size distribution prevailing at or near the nozzle and the drying characteristics of the feed solution, it is felt that a spray drying chamber can now be designed with reasonable confidence on the basis of the methodology presented here. The latter is obviously preliminary in nature but is readily amenable to improvement as experience in its use is gained. Although the chamber geometry considered here is at first sight simpler than some of the industrial cases, which may incorporate additional complexities such as multiple air inlets, multiple atomizing nozzles, countercurrent flow, etc., it is important to remember that the present program can be easily modified to take such complexities into account.

When dealing with multiphase flows, one is always faced with the difficult problem of accounting for the momentum, mass, and energy couplings between phases. The exact analysis of these flows in three-dimensional motion becomes enormously complex. Fortunately, the droplet and/or particle loading in spray drying operations is so low that the coupling effects between phases are negligibly small. Accordingly, they have been neglected in the present treatment.

Finally, the lack of information on vortex flow fields has also been until now one of the most difficult problems in the design of spray dryers. Based on the experimental evidence obtained in the course of a study of the flow patterns in the same type of chamber as considered here, it is now possible to use the following correlations to predict the tangential and axial velocity distributions, respectively:

$$V_{at} = C_1 \, (r/R_x)^{0.5}$$

$$V_{av} = C_3 \, (r/R_x)^{2.5}$$

where C_1 and C_3 are constants which depend on the axial distance from the roof of the chamber and the volumetric flow rate of the drying gas at the inlet. The width of the annular region where the tangential velocity decreases steeply to zero was found to be approximately constant. The radial velocities were found to be negligible.

The present investigation has shown that, for the case chosen, the drying period can be correlated to the droplet diameter. If experience shows that such a correlation exists for other chamber geometries as well, the design calculations can be considerably simplified. The design of a dryer then requires the calculation of the droplet trajectory only. The following correlation was obtained for the drying period as a function of the droplet diameter for the operating conditions chosen in this study:

$$\tau = 1.04 \times 10^{-4} \, (d_i)^{1.87} \text{ s}$$

In 1954, Marshall presented what was to remain one of the most comprehensive reports on many aspects of spray drying for the next two decades. Recently, the whole field was thoroughly reviewed by Mochida and Kukita (1971 to 73) in a series of twenty-three articles, with emphasis on the theoretical aspects, and by Masters (1972), with emphasis on industrial practice. It is significant to note that to date no generalized design method has emerged from the hundreds of papers cited in these two reviews. Since the latter were published, only a few studies, pertinent to spray dryer design, have appeared in the literature, which shall now be briefly summarized.

One of the most important aspects of spray dryer design is the estimation of droplet trajectories. Bailey, Slater, and Eisenklam (1970) predicted droplet trajectories for some simple cases in a vortex flow considering the interaction of heat transfer and mass transfer at high temperatures. More recently, Domingos and Roriz (1974) computed

droplet trajectories in swirling flows with and without recirculation. The flow field was also computed in some of the examples. They found that the effect of lift was slight, and the added mass due to acceleration was negligible.

Fabian (1974) studied analytically the trajectories of small spherical particles in various free vortex flow fields with a view to describing the operation of centrifugal particle separators and to assist in their design. The flow field was also computed for both laminar and turbulent boundary layers on a conical convergent nozzle with swirling throughflow.

The lack of information on flow patterns has also been a major difficulty in spray dryer design. Schowalter and Johnstone (1960) carried out detailed measurements in a vortex tube which provided a good picture of the flow field, but the authors made no effort to correlate their results. Paris et al. (1971) developed a model of the air flow in a countercurrent spray drying tower by deconvolution of the residence-time distribution data obtained by means of a helium tracer. The significance of the model is that it corresponds to the actual operating conditions in the presence of the spray.

Recently, Bank (1975) in this laboratory made extensive measurements of mean velocities and turbulence intensities in a confined vortex flow by means of hot wire anemometry. These results are discussed in detail later in the section on flow patterns.

Janda (1973) measured the tangential velocities of air by means of a spherical probe in the cylindrical portion of a spray drying chamber with a conical bottom; the chamber was equipped with a centrifugal disk atomizer at the top, near which the drying air was introduced tangentially. He obtained the following correlation:

$$V_{at} = a/r^b \qquad (1)$$

where b was found to have a value of 0.77 and a varied from 630 down to 210, depending on the setting of the distribution flap. However, the value of the inlet tangential velocity was not given. He mentioned that the flap is normally set so that a has a value of 350. In spite of many simplifying assumptions, the design correlations he proposed for this type of chamber were experimentally verified.

Sen (1973) carried out a mathematical modeling of the spray drying process by both the distributed parameter and the lumped parameter techniques in an effort to study the steady, and unsteady, state behavior of the system. Experimental studies were also conducted to obtain the transient response of the outlet temperature from an exponential change in the temperature of the inlet gas. The experimental results showed that the steady state temperature distributions within a spray dryer lie between those predicted by the distributed and lumped parameter models.

Very recently, Crowe et al. (1975) presented an analysis of two-dimensional gas-droplet flows in which the effects of mass, momentum, and energy couplings between the two phases were accounted for by using the concept of regarding the droplet phase as a source of mass, momentum, and energy to the gaseous phase. They called this concept the Particle-Source-in-Cell (PSI-Cell) model. In an earlier paper, Crowe and Pratt (1974) had applied this model to the two-dimensional analysis of the flow field in cyclone separators, which successfully predicted the well-known increase in collection efficiency with increased dust loading. There is no doubt that this model is conceptually more rigorous than the one developed in this paper. However, its application to three-dimensional motion would become extremely complex and would still require the use of experimentally obtained parameters. In addition, in the special case of spray drying, the loading of the condensed phase is so low that the coupling effects are negligibly small. As far as momentum coupling is concerned, for example, Rao and Dukler (1971) have demonstrated by means of a momentum probe of new design that the velocity profile of air flow in ducts was not affected by particle loadings considerably larger than those encountered in spray dryers.

The approach used in the present work is basically a Lagrangian one, whereby the evaporating droplets are coupled by means of heat and mass transfer relations to the entraining drying air in their three-dimensional trajectories. In spite of the large number of simultaneous equations involved, the use of experimental correlating coefficients keeps the computational program down to a manageable size.

EXPERIMENTAL

Velocity measurements were carried out in a chamber typical of a concurrent, vertical, downflow type of spray dryer with tangential air entry. The chamber consisted of 1.22 m I.D. × 0.61 m high upper jacketed cylindrical section and a 1.22 m high lower conical section. Air from the blower was introduced tangentially into a 5.1 cm wide annular jacket surrounding the cylindrical section and then distributed to the chamber through six slots (3.8 × 15.2 cm) cut in the inside wall at an angle of 45 deg. to the direction of the airflow. The metal was not cut out but merely bent back along a 90 deg. edge. Hot wire anemometry was employed to measure mean velocities and turbulence intensities. The experimental results are presented below in the section on air flow patterns.

BASIC DESIGN EQUATIONS

In this section, all the basic equations required for the proposed design methodology will be presented. Most of these equations are based on published experimental data. No effort has been made, however, to present an exhaustive review of all available information. As better data appear in the literature, they can be easily incorporated in the final program. To give the treatment more generality, all three modes of atomization will be considered, as far as they affect the design methodology.

Atomization

Atomization is the most important process in the spray drying operation, since it governs the size of the product, and the initial drop size distribution of the spray generated by the atomizer forms the basis of the chamber design. The three principal types of atomizers used today are centrifugal disk atomizers, pressure nozzles, and pneumatic nozzles. Centrifugal disk atomizers are generally employed for high capacities owing to their flexibility and ease of maintenance. Pressure nozzles are preferred for highly viscous feeds and where multiple atomizers are desired. Pneumatic nozzles are used only for small capacities due to the high cost of compressed air and their low efficiency. The above three atomizers will now be discussed in terms of the droplet size distribution (DSD) and of the largest droplet diameter they generate. Although the correlations which will be presented are useful for preliminary design calculations and provide a good approximation of the DSD to be expected from a given type of atomizer, there is no substitute for the information obtained from tests with the actual atomizer in conjunction with the actual feed solution to be dried.

Centrifugal Disk Atomizers. Centrifugal disk atomizers are by far the most commonly used atomizers today. Masters (1972) presented a large number of correlations available in the literature to predict DSD from various

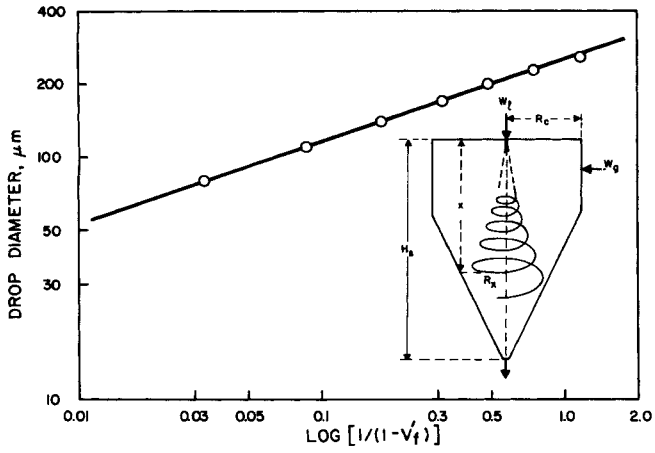

Fig. 1. Droplet diameter as a function of log $[1/(1 - V'_f)]$. (Shown as an insert is the chamber geometry considered as an illustration of the design methodology.)

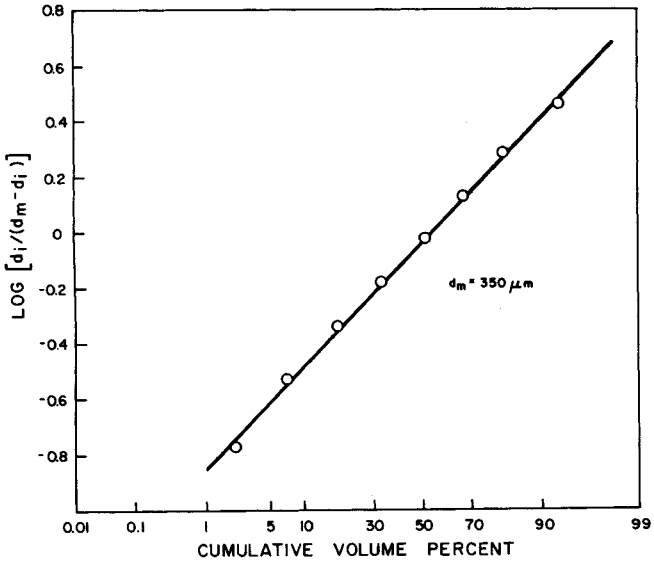

Fig. 2. Log $[d_i/(d_m - d_i)]$ as a function of cumulative volume percent.

types of such atomizers. A very useful correlation is that obtained by Friedman et al. (1952). They correlated the Sauter mean diameter to the disk radius in terms of dimensionless groups to obtain

$$\frac{d_{vs}}{R_d} = 0.4 \left(\frac{G}{\rho_f N R_d^2}\right)^{0.6} \left(\frac{\mu}{G}\right)^{0.2} \left(\frac{\sigma \rho_f L_w}{G^2}\right)^{0.1} \quad (2)$$

They found the following relationship between the largest droplet size and the Sauter mean diameter:

$$d_m = 3\, d_{vs} \quad (3)$$

Pressure Nozzles. The drop size distribution from pressure nozzles has been found (Marshall, 1954) to follow the Rosin-Rammler relationship

$$1 - V_f' = \exp\left[-0.693\, (d_i/d_p)^{\delta}\right] \quad (4)$$

where d_p is the particle diameter above which 36.79% of the volume or mass of the spray has drops of larger diameters, and δ is a constant which depends on the uniformity of the spray. Sauter mean diameter d_{vs} and d_p are related by

$$d_{vs} = d_p/\Gamma(1 - 1/\delta) \quad (5)$$

Several correlations are available in the literature to predict the mean droplet size from various types of centrifugal pressure nozzles (Masters, 1972).

Pneumatic Nozzles. The drop size distribution from pneumatic nozzles has been shown to follow (Nukiyama and Tanasawa, 1938 to 40)

$$n_i/\Delta d = a d_i^2 \exp\left(-b d_i^q\right) \quad (6)$$

where q was shown to be a constant for a given nozzle and should be determined experimentally.

From a mathematical analysis, Nukiyama and Tanasawa determined the relations between the constants a and b and d_{vs} for different values of q. The following relations were presented when q had a value of 2:

$$b = 2.25/d_{vs}^2 \quad \text{and} \quad a = 1.91 b^3 V \quad (7)$$

Based on the novel experimental technique of spray cooling molten wax or melts of wax-polyethylene mixtures, Kim and Marshall (1971) proposed the following volume frequency function for droplets produced by pneumatic atomizers:

$$V_f' = [16.7 \exp(-2.18\, d/\bar{d})]/ [1 + 6.67 \exp(-2.18\, d/\bar{d})]^2 \quad (8)$$

where $\bar{d}$, the mass median diameter, is given by the following empirical equation for a conventional single-air entrance atomizer:

$$\bar{d} = 160.8\, \sigma^{0.41} \mu^{0.32}/(V_{rel}^2 \rho_a)^{0.53} A^{0.36} \rho_f^{0.16} + 1\,573\, (\mu^2/\rho_f \sigma)^{0.17} (W_A/W_1)^n/V_{rel}^{0.54} \quad (9)$$

Here $n = -1$, if $(W_A/W_1) < 3$, and $n = -0.5$, if $(W_A/W_1) > 3$. The coefficients in Equation (9) have been recalculated to account for the conversion to the units used in the present paper.

Although pneumatic atomizers are seldom used in large-scale industrial applications, these equations are nonetheless very useful because of the frequent use of this type of atomizing device for preliminary testing of the drying characteristics of a feed material. It is to be noted that Equation (9) includes certain parameters which are characteristic of the nozzle design and in this way differs from Nukiyama and Tanasawa's well-known equation. The same authors also presented a slightly modified form of Equation (9) to predict the value of $\bar{d}$ in the case of a concentric double-air nozzle atomizer.

The Largest Drop Diameter. Mugele and Evans (1951) proposed a special upper-limit function $\ln[a d_i/(d_m - d_i)]$ for describing droplet size distributions in sprays. They observed that this function fitted accurately the available spray data obtained on all three types of nozzles, although it is not capable of predicting by itself the DSD of a given atomizer. In this method, the largest droplet diameter d_m is obtained by a trial-and-error procedure from the best fit when $\ln[d_i/(d_m - d_i)]$ is plotted against cumulative number or volume frequency. Recently, Katta and Gauvin (1975) showed this analytical method to give values of d_m in excellent agreement with the experimental results.

As an illustration, Figure 1 represents the DSD [plotted according to Equation (4)] of the centrifugal pressure nozzle (Type 3/8 A 10 Spraying Systems Co., Wheaton, Ill.) which was selected for the design problem which will be discussed later in this paper (a sketch of the spray drying chamber used in the latter is shown as an insert). When operated at 1 000 lb/sq in. pressure, the DSD supplied by the manufacturer is

d_i, μm	50	80	110	140	170	200	230	260	290
Cumulative volume, %	2.2	7.3	18	33	51	67	81	93	100

From the Mugele and Evans method, a value of 350 μm for the largest drop diameter d_m gave the best fit when their upper-limit function was plotted on a probability grid. The adequacy of the fit is illustrated in Figure 2.

Droplet Trajectories

The three-dimensional equations of motion of a droplet in centrifugal and gravitational fields can be written as

$$dV_t/dt = -V_tV_r/r - 3C_D\rho_aV_f(V_t - V_{at})/4d_i\rho \quad (10)$$

$$dV_r/dt = V_t^2/r - 3C_D\rho_aV_f(V_r - V_{ar})/4d_i\rho + F_L/m \quad (11)$$

$$dV_v/dt = g - 3C_D\rho_aV_f(V_v - V_{av})/4d_i\rho \quad (12)$$

where V_f, the velocity of the droplet relative to the fluid, is given by

$$V_f^2 = (V_t - V_{at})^2 + (V_v - V_{av})^2 + (V_r - V_{ar})^2 \quad (13)$$

The drag coefficient was determined by means of the equations presented by Beard and Pruppacher (1969), which, in the authors' judgment, are the most correct.

The shear lift force on the droplets was estimated by means of

$$F_L = 20.25\,\rho_a d_i^2\,(v_a/K)^{0.5}\,KV_f \quad (14)$$

where:

$$K = 1.4\,V_{av}\,(r/r_5^2) \quad (15)$$

The above equations of motion are to be solved simultaneously with the equations expressing the instantaneous evaporation rate of the droplets, the three-dimensional drying air flow pattern, and the instantaneous properties of the drying gas. The latter will now be discussed in turn.

Evaporation and Drying

The heat and mass transfer rates to the droplets are given by

$$dq_i/dt_i = \pi k_a Nu\, d_i\, n_i\,(t_a - t_s) \quad (16)$$

$$dm_i/dt_i = \pi D_v\rho_a d_i Sh\, n_i\,(H_w - H) \quad (17)$$

where the Nusselt and Sherwood numbers were calculated from the following equations:

$$Nu = 2.0 + 0.6\,(Re)^{0.5}\,(Pr)^{0.33} \quad (18)$$

$$Sh = 2.0 + 0.6\,(Re)^{0.5}\,(Sc)^{0.33} \quad (19)$$

The saturation humidity was obtained from

$$H_w = 18\,p_w/29(p_t - p_w) \quad (20)$$

The effect of high temperature of the drying gas on mass transfer rates was taken into account by means of the correction factor $a'/(e^{a'} - 1)$, where a' is given by

$$a' = \ln\,[1 + (Nu\cdot\Delta T\cdot C_p/2\lambda)] \quad (21)$$

The actual evaporation rate is equal to the apparent evaporation rate multiplied by $a'/(e^{a'} - 1)$.

The effect of heat losses should be taken into account in calculating the rate of evaporation and/or drying rate. As shown in Figure 3 (upper figure, in the case of pure water or of a colloidal solution), if the heat losses are negligible, the temperature of the droplets follows the adiabatic cooling curve (path 1-2). On the other hand, if they are appreciable, the driving force is reduced accordingly (path 1-3).

In the case of an actual solution, as shown in the lower diagram of Figure 3 (assuming no heat losses for simplicity), the drying rate is also affected by the change in solid concentration of the droplets (which results in an increase of their surface temperatures to T_{w2}, T_{w3}, etc.), by the change in latent heat of vaporization with the droplet temperature, and by the heat of crystallization. If the latent heat of vaporization increases significantly due to the heat of adsorption in the last stages of drying, the adiabatic saturation curve, and consequently the path of the air point, will be deflected downward as shown by the lower dotted line. But, on the other hand, if, during the drying of a salt solution, heat of crystallization is released, the adiabatic saturation curve will be deflected upward, as shown by the upper dotted line. In most cases, it is likely that both situations would occur simultaneously, and the net effect on the drying rate would not be significant. At all events, the absolute values of the changes caused by these two phenomena are not large.

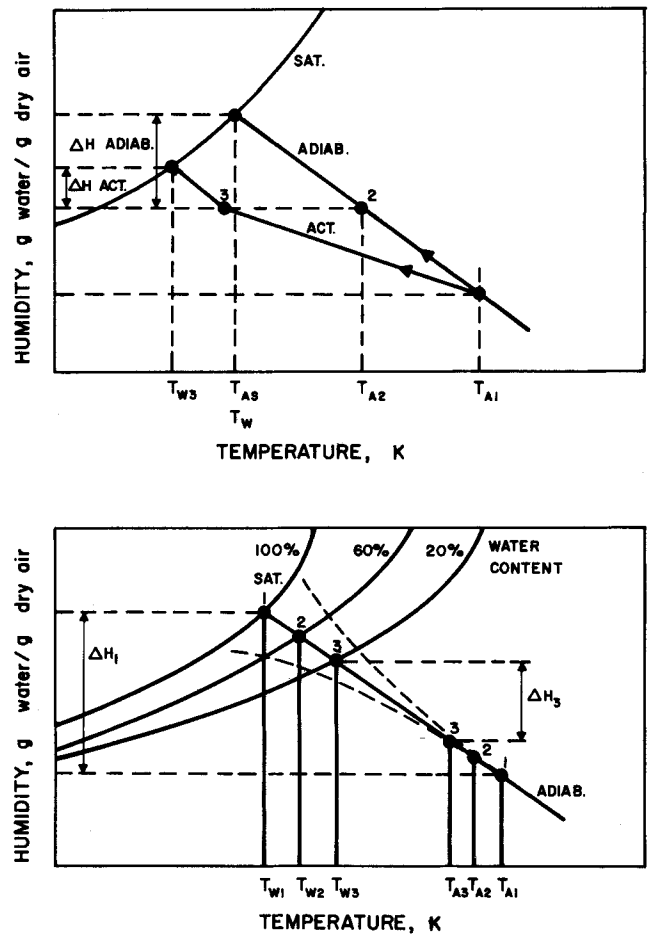

Fig. 3. Psychrometric chart.

The above considerations apply strictly if the increase in concentration is uniform throughout the droplet as it dries. Because of the extremely high rate of evaporation, Ranz and Marshall (1952) indicated that the droplets evaporated as though their surface were at the saturation concentration corresponding to their wet bulb temperature. Although the drying behavior of small atomized droplets can be expected to be different from that of the large drops studied by these authors, this assertion is supported by the observations of Baltas and Gauvin (1969*c*) on the complex phenomena accompanying the crystallization of spray dried sodium nitrate (which is the feed material considered in the illustrative problem to be discussed later). These authors noted that at low drying air temperatures, small crystallites formed inside the droplets; at intermediate temperatures, surface crust formation was observed. At still higher temperatures, the work of a number of authors would indicate that hollow particles of large diameter, with wall thickness of 5 to 10 μ, could be formed. As a preliminary design consideration, the assumption of surface saturated condition and neglect of a

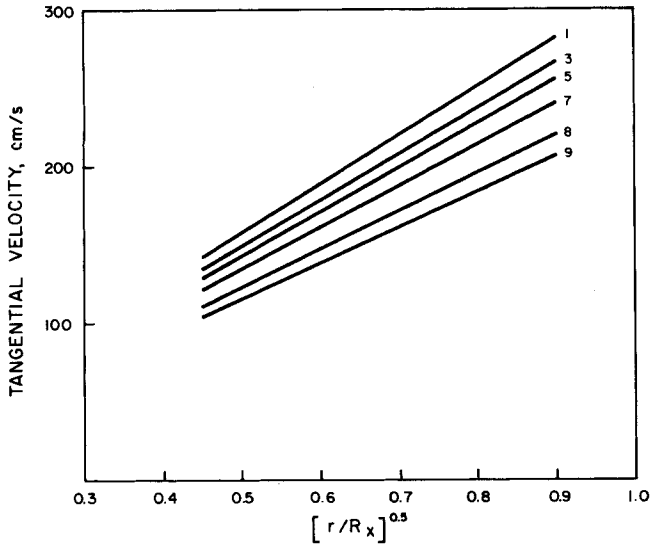

Fig. 4. Tangential velocity of the gas as a function of $[r/R_x]^{0.5}$.

drying falling rate period, with resulting constant droplet surface temperature, is probably adequate.

Finally, the instantaneous diameter of any droplet was obtained from the following equation based on the assumption that the droplets are dense:

$$d_i = d_{in}\,(\rho_{in}c_{in}/c_i\rho_i)^{0.33} \qquad (22)$$

where the subscripts i and in represent the instantaneous values and the initial values, respectively, of the same droplet class.

Air Flow Patterns

Nozzle Zone. The zone traversed by the droplets as they decelerate from their high initial velocity to the point where they begin to be entrained by the swirling drying gas is designated as the nozzle zone, since in that region the droplets are mostly affected by the atomizing nozzle. It is also characterized by the large amount of drying gas which is entrained into it from the surroundings. The gas flow patterns within the spray were shown to be similar to those in a gas jet by Rasbash and Stark (1962), Gluckert (1962), Briffa and Dombrowski (1966) and Benatt and Eisenklam (1969) who studied the properties of sprays in detail.

In the case of a pressure nozzle, the decay of the center line velocity of the gas within the spray can be correlated by the following equations based on the work carried out by Gluckert (1962) and Briffa and Dombrowski (1966):

$$V_c/V_o = 3.2\,(D_o/x) \qquad (23)$$

$$V_o = W_1/(\rho_f A_1) \qquad (24)$$

where V_o is the average velocity of the liquid leaving the pressure nozzle and A_1 is the cross-sectional area available for liquid flow at the nozzle. The radius of the air core can be estimated to be half the radius of the nozzle on the basis of the results correlated by Nelson and Stevens (1961) showing the effect of the spray angle on the air core.

In the case of a centrifugal disk atomizer, Gluckert (1962) presented the following equations from an experimental study:

$$V_c/V_o = 1.2\,[b'/(r - R_d)]^{1/2}\,(r/R_d)^{1/2} \qquad (25)$$

$$b' = W_1/[\sqrt{2}\cdot(2\pi R_d)^2 N\rho_{a2}] \qquad (26)$$

where b' is the width of an imaginary annular jet of gas (of same composition as that leaving the spray dryer) having the same velocity and momentum as the initial liquid jet.

For pneumatic nozzles, it has been reported earlier (Katta and Gauvin, 1975) that the following equations apply to the center line velocity:

$$V_c/V_o = 6.5/\bar{x} \qquad (27)$$

$$\bar{x} = (\rho_\alpha/\rho_o)^{0.5}\,(x/D_o) \qquad (28)$$

It is generally accepted that the induced air jet in the case of a pressure nozzle can be assumed to behave like a free jet. On this basis, the radial distribution of the axial velocity is represented by

$$V_{av} = V_c \exp[-0.692(r/r_5)^2] \qquad (29)$$

where the variation of r_5 with the axial distance depends on the angle of the spray. For a free jet or a spray from a pneumatic nozzle, the angle of the cone formed by the boundary is about 20 deg. If the half angle of the cone formed by the locus of the half center line velocities (half speed cone) is taken as 5 deg., r_5 is given by

$$r_5 = x\tan 5^\circ = 0.0873\,x \qquad (30)$$

The experimental work of many investigators agrees with this expression. By assuming that the analogy will hold far larger spray angles, the following is obtained for a 60 deg. spray angle:

$$r_5 = x\tan 15^\circ = 0.268\,x \qquad (31)$$

The radial velocities of the induced air jet were taken as zero on the basis of the work carried out by Benatt and Eisenklam (1969).

Free Entrainment Zone. The zone where the droplet motion is unaffected by the atomizing nozzle and is governed by the entraining drying gas only is designated as the free entrainment zone. The tangential velocities obtained experimentally by Bank (1975), in the spray-drying chamber described earlier, were represented by

$$V_{at} = C_1\,(r/R_x)^{0.5} \qquad (32)$$

where C_1 is a constant which depends on the axial distance from the roof. The values of C_1 as a function of the dimensionless axial distance are given in the following table:

x/H_s	0.27	0.41	0.52	0.68	0.79	0.85
C_1, cm/s	315	298	286	269	245	231

The experimental tangential velocity profiles are shown in Figure 4 at various stations, the locations of which are given in the following table:

Station	1	2	3	4	5
x/H_s	0.274	0.351	0.406	0.462	0.517
Station	6	7	8	9	
x/H_s	0.6	0.684	0.768	0.851	

The radius of the chamber at any axial distance x from the roof of the chamber (see Figure 1) in the conical portion can be obtained from

$$R_x = 1.469\,R_c - 0.469x \qquad (33)$$

The tangential velocities in the annular region can be represented by

$$V_{at} = C_2(R_x - r) \qquad (34)$$

where C_2 is given by

$$C_2 = 61\,C_4/R_c \qquad (34a)$$

The value of C_4 was obtained from experimental data and was determined to be 80 cm/s.

The radius of the annular region was obtained from

$$r_m = R_x - 0.05\,R_c \tag{35}$$

Bank measured the flow angles experimentally. With increasing axial distance from the roof, the flow angle increased to about 15 deg. and then became steady at a x/H_s ratio of 0.6. This indicates that in the major portion of the conical bottom, the flow consists of almost parallel circular streamlines. It is important to remember, in this connection, that Bank observed that the flow patterns were not affected by the entrance volumetric flow rate.

The axial velocities reported by Bank, as shown in Figure 5, can be represented by

$$V_{av} = C_3(r/R_x)^{2.5} \tag{36}$$

where C_3 is a constant which depends on the axial distance. By integrating the above velocity profile across any cross section of the chamber, the following value of C_3 was obtained:

$$C_3 = 2.25\,W_g/(\rho\pi R_x^2)$$

or

$$C_3 = 2.25\,\overline{V}_{av} \tag{37}$$

The radial velocities were taken to be zero, as Bank has experimentally shown that they are negligibly small.

It should be noted that the above equations will hold only if the drying air is introduced from a single tangential inlet near the top of the chamber, or from well-distributed multiple inlets into the drying chamber from a surrounding plenum chamber. They will not strictly apply if the drying air is given an initial strong downward velocity component, as was observed by Gauvin et al. (1975).

The entrainment rates in the nozzle zone of a pressure atomizer can be obtained from the following correlation presented by Benatt and Eisenklam (1969) based on both experimental and theoretical studies:

$$E = M_e/[(x - x')\sqrt{W_1 V_o \rho_a}] \tag{38}$$

where

$$x' = 0.5 + 1.66(W_1/\rho_1\sqrt{p_1})^{0.5}\cos\theta \tag{39}$$

and E, the entrainment parameter, is given by

$$E = 0.96\tan\theta/\sqrt{\cos\theta} \tag{40}$$

In the case of pneumatic nozzles, it has been reported in earlier studies that the entrainment rate is given by

$$M_e = M_o[0.23(x/D_o) - 1] \tag{41}$$

Properties of Drying Gas

The amount of drying air W_g needed can be estimated from the following overall energy balance on the spray drying chamber over the datum t_w:

$$W_g C_s(t_1 - t_2) = W_w\lambda + W_w C_f(t_2 - t_w) + W_1 C_f(t_w - t_f) + W_p C_{ps}(t_p - t_w) + q_1 \tag{42}$$

The temperature of the drying gas in the nozzle zone is obtained from an energy balance in this zone:

$$(t_1 - t_x) = [E_x\lambda + W_p C_{ps}(t_p - t_w) + q_{1x}]/(M_e C_{s1}) \tag{43}$$

The average humidity at any section is determined from the rate of evaporation and the rate of entrainment:

$$H_x = (E_x/M_e) + H_1 \tag{44}$$

The temperature of the drying gas in the free entrainment zone can be calculated from the following energy balance between the inlet and the section under consideration:

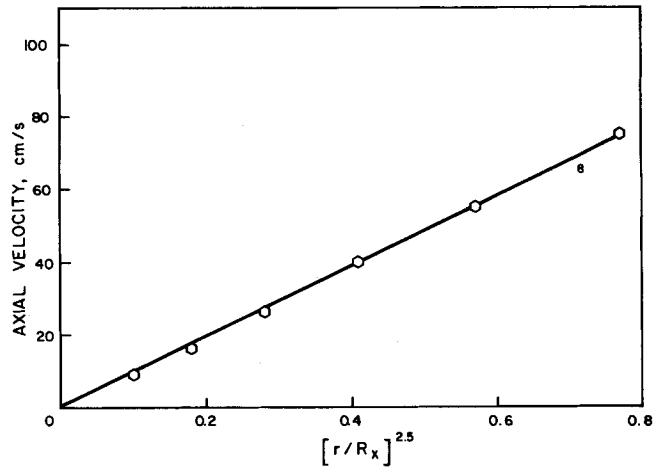

Fig. 5. Axial velocity of the gas as a function of $[r/R_x]^{2.5}$.

$$(t_1 - t_x) = [E_x\lambda + (E_x - W_p)(t_2 - t_w)C_f + q_{1x} + W_p C_{ps}(t_p - t_w)]/(W_g \cdot C_s) \tag{45}$$

The average humidity in this zone is obtained from the flow rate of the drying gas and the rate of evaporation:

$$H_x = (E_x/W_g) + H_1 \tag{46}$$

It was assumed that the radial temperature and humidity gradients in the drying gas are negligible. The heat losses were first calculated for the whole chamber by using an overall heat transfer coefficient. For any given section of the chamber, it was then assumed that the heat losses were proportional to the extent of evaporation. It can be seen that the above equations include the amount of heat supplied to the solids, a relatively small item.

Methodology of Design

General Considerations. When a spray dryer is designed, the required rate of production of powder, together with the product specifications (particle size distribution, bulk density, and residual moisture content), are given. The product specifications are usually determined from small-scale trials in an experimental spray dryer, unless this information is available from the literature. Similarly, the physical and chemical properties of the feed solution are known, from which the psychrometric charts shown in Figure 3 can be determined. If the product is heat sensitive and/or prone to oxidation, careful attention must be given to the temperature profile of the drying air in the chamber, since the temperature of a particle of product will rise rapidly towards that of the surrounding gas once its moisture has been driven off. This will obviously occur much sooner in the case of the droplets of initially smaller diameters. All these considerations, as well as the selection of an appropriate chamber geometry resulting from them, have been fully discussed by Masters (1972) and will not be further elaborated here.

Design Criteria. An important consideration in spray dryer design is the selection of a suitable criterion against which the adequacy of the design results can be tested. A number of such criteria suggest themselves, such as the attainment of a specified humidity and temperature in the exit gas, attainment of a given moisture content for a specified fraction of the DSD in a specified zone of the chamber, maximum thermal efficiency, etc.

The criterion selected in the present design method requires that the largest droplet in the initial spray shall be dry (or will have reached the specified nonsticky

Table 1. Specifications and Requirements

Rate of production	1 000 kg/h
Percent $NaNO_3$ in feed	30%
Residual moisture content of the largest size	10%
d_{vs} of product (assumed dense)	95 μm
Inlet temperature of drying air	650°K
Drying air inlet humidity	0.005
Ambient temperature	294°K
Wet bulb temperature of drying air	333°K
Density of feed solution	0.922 + (0.92) (c_i)

Table 2. Atomizing Nozzle Specifications

Nozzle type	Centrifugal pressure nozzle
Model number	3/8 A 10
Nozzle manufacturer	Spraying Systems Co.
Operating pressure	689.5 N/cm^2 (1 000 lb/sq.in.abs.)
Diameter of nozzle	0.476 cm
Liquid velocity at nozzle	169 m/s
Angle of the spray	60 deg.
DSD of spray	Shown in Figure 1
Diameter of largest droplet	350 μm (Figure 2)

Table 3. Results of Design Calculations

Height of chamber	15 m
Diameter of cylindrical section	10 m
Height of cylindrical section	5 m
Drying air mass flow rate	9.267 kg/s
Average tangential velocity of drying air at inlet	3.20 m/s
Cross-sectional area of inlet	5.3 m^2
Volumetric flow rate of drying air	16.94 m^3/s
Total heat required	2.3×10^6 J/s
Initial velocity of droplets	2 d_i + 600 cm/s
Outlet temperature of drying air	422°K
Overall heat transfer coefficient for estimation of heat losses	5.9 J/m^2 · s · K
Heat losses	0.47×10^6 J/s (20.6%)
Thermal efficiency	48%

residual moisture content) before it reaches the chamber wall. This criterion lends itself particularly well to the computational approach proposed below. It also has the practical advantage of providing against the accumulation of wet powder on the walls, which is an inherent problem in the operation of spray dryers. It is realized, on the other hand, that it will lead to chamber sizes which may be considered overconservative for practical purposes. As experience with this design method accumulates, however, this criterion may be relaxed as required by simply decreasing the upper limit of the initial droplet size, on which the design calculations are based.

Method of Calculations. The design of a spray dryer is therefore carried out in the following steps:

1. From the desired product size distribution and the nature of the product, the DSD near the nozzle for an optimum concentration of the feed is determined, and then the largest droplet size is predicted.
2. The drying gas flow patterns and the type of chamber are selected on the basis of the nature of the product and the drying characteristics of the feed solution.
3. The droplet trajectories both in the nozzle and entrainment zones are calculated with the help of a computer by using the numerical approach suggested here. Reasonable values for the size of the dryer and inlet velocity have to be assumed initially.
4. The calculations are repeated until the dryer dimensions are just adequate to dry the largest droplet.

It will be recalled that the computational approach followed here was used in two earlier studies (Gauvin et al., 1975, and Katta and Gauvin, 1975) to predict successfully the droplet trajectories in an experimental spray drying chamber.

In the illustrative design problem which follows below, the computations were done on an IBM 360/75 computer. Since all the equations have to be solved simultaneously, the same axial distance step and a variable time step were used for all classes of droplets so that they would advance to the same plane perpendicular to the dryer axis. The largest time increment used was 10^{-3} s initially and 10^{-2} s for most of the remaining calculations. These calculations were repeated for various sizes of dryers until the dryer, which is just adequate to dry the largest droplet, was obtained.

EXAMPLE OF SPRAY DRYER DESIGN

Application of the above concepts to the design of an industrial size spray dryer will now be described. The material to be spray dried consists of a 30% solution of sodium nitrate. Table 1 lists the product specifications and various requirements to be met.

Additional information concerning the properties of the feed and its drying characteristics can be found in the work of Baltas and Gauvin (1969*a, b, c*) who studied this system in detail. By assuming heat losses of 20% (which from Table 3 is roughly correct), the psychometric charts shown in Figure 3, in conjunction with the solubility data for sodium nitrate solution from the Landolt-Börnstein Tables, give a droplet temperature of about 363°K and a saturated concentration of 61%, both of which are assumed to remain constant during the drying process.

Based on the product size requirements, a centrifugal pressure nozzle was selected as the atomizer. Specifications for this nozzle are given in Table 2.

A concurrent vertical downflow chamber with a cylindrical top section and a conical bottom section was chosen for this application because of its known flow patterns. The drying air enters the top section tangentially, and the height of the conical section is twice that of the cylindrical one (Figure 1).

The initial conditions chosen for the computations corresponded to a plane at 20 cm from the nozzle exit. Based on the work of York and Stubbs (1952), the initial droplet velocities were derived. Eight classes of initial droplet sizes were chosen for this study. The positions of the droplet classes, as they were unknown, were assumed to be in an arithmetic progression from the center to the edge of the spray, with the largest size class being at the edge of the spray.

The efficiency of the spray drying operation is best defined as the ratio of the heat used in vaporization to the total heat available and can be shown to be equivalent to the following:

$$\eta = W_w\lambda/[W_g(t_1 - t_w)C_{s1} + W_1(t_f - t_w)C_f] \quad (47)$$

Table 3 presents a summary of the results of the design calculations.

Comments concerning the calculations and discussions of some of the intermediate results obtained in their course will now be presented, as they provide an interesting insight into the spray drying operation.

As mentioned earlier, entrainment from the surrounding drying gas is one of the major characteristics of the nozzle zone. If the latter is viewed in this light, it enables proper comparison between the three principal types of atomizers. The drop trajectory calculations in the nozzle zone depend on the rate of entrainment, in addition to the flow patterns

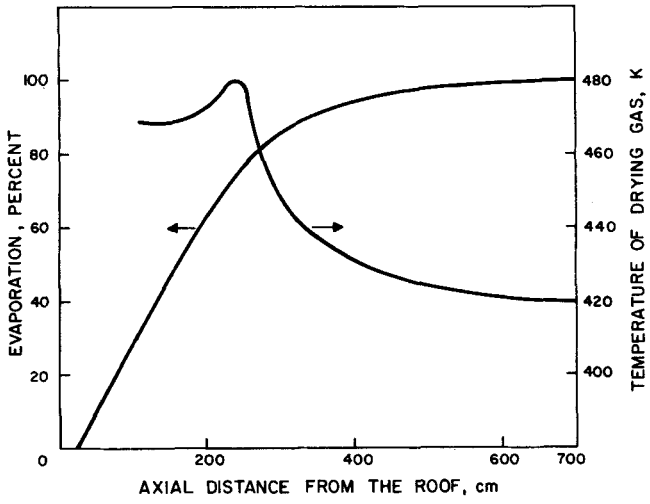

Fig. 6. Evaporation rate and the temperature of the drying gas as a function of the axial distance from the roof.

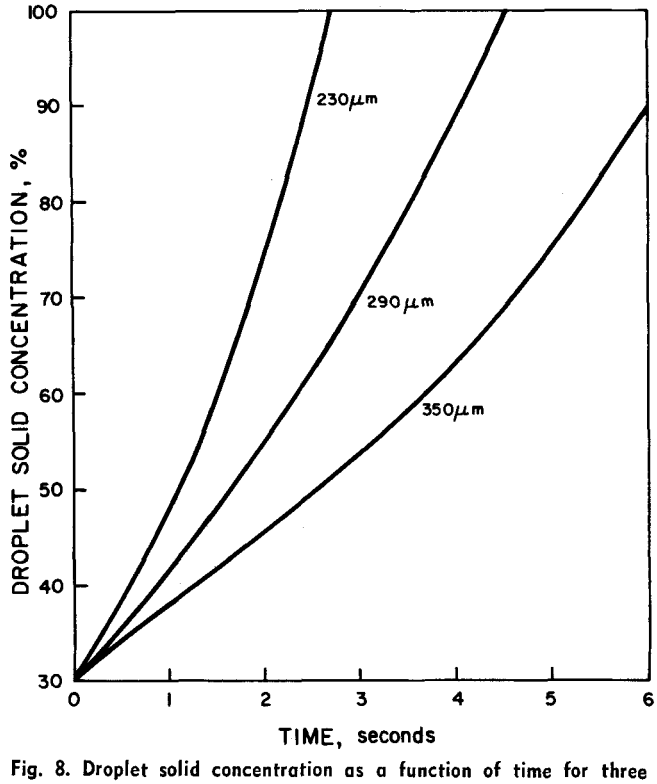

Fig. 8. Droplet solid concentration as a function of time for three different sizes.

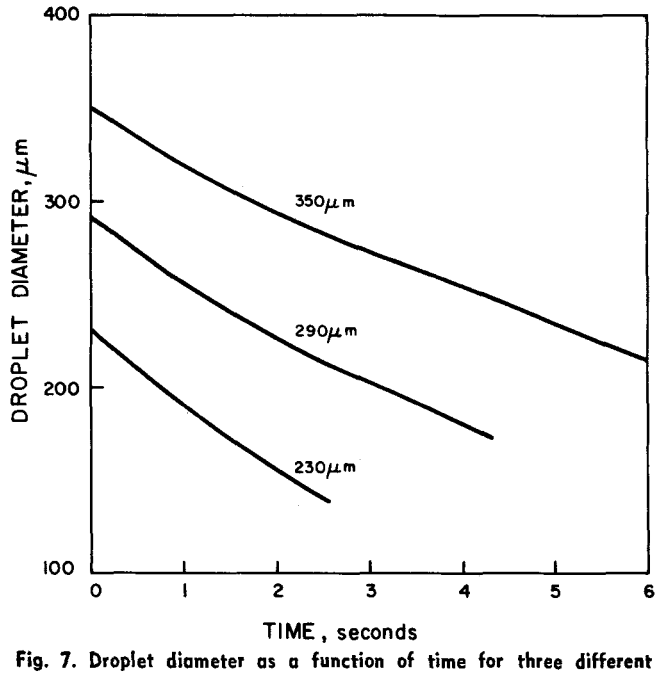

Fig. 7. Droplet diameter as a function of time for three different sizes.

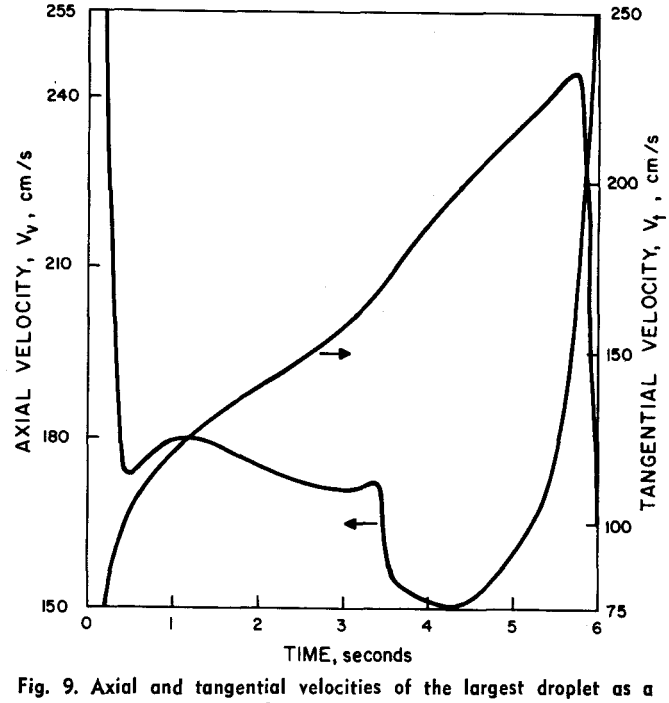

Fig. 9. Axial and tangential velocities of the largest droplet as a function of time.

within the spray. Hence these calculations depend on the type of atomizer used. On the other hand, the drop trajectory calculations in the free entrainment zone depend on the flow patterns of the drying gas and not on the type of atomizer used to any significant extent.

According to the above definition of the nozzle zone, the amount of evaporation in this zone is about 80%, as can be seen from Figure 6 and Equation (38) which gives the rate of entrainment. This clearly indicates the importance of the nozzle zone in the design of spray dryers.

The average temperature of the drying gas within the spray in the nozzle zone and in the free entrainment zone is also shown in Figure 6. The increase in the gas temperature after the initial decrease is due to entrainment from the surrounding hotter gas. Most of the decrease in the gas temperature takes place in the nozzle zone and is due to the high evaporation rates.

The change in droplet diameter with time is shown in Figure 7. The variation of droplet solid concentration with time for three initial sizes is shown in Figure 8. The larger droplets reach higher concentrations at a much slower rate than the smaller droplets, as can be expected.

Figure 9 gives the axial and tangential velocities of the 350 μm (initially) droplet as a function of time. The initial decrease of the axial velocity is due to the decreasing gas velocities in the nozzle zone. It is followed by small changes in the velocity over a large part of its residence time and then increases due to the converging flow field in the conical section of the chamber. The ever increasing tangential velocity of the droplet until it comes close to the chamber wall is due to the fact that the gas tangential velocity increases as the droplet moves away from the axis of the dryer and into the conical section. When the droplet enters the boundary layer at the wall,

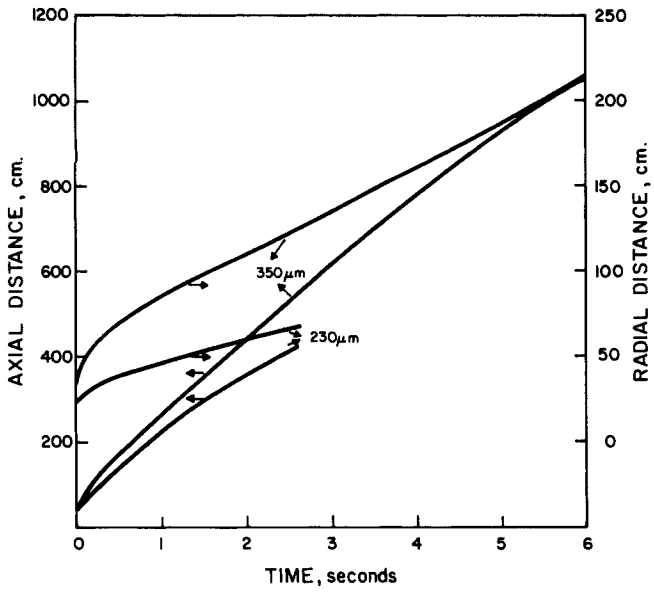

Fig. 10. Axial and radial locations of the largest droplet as a function of time.

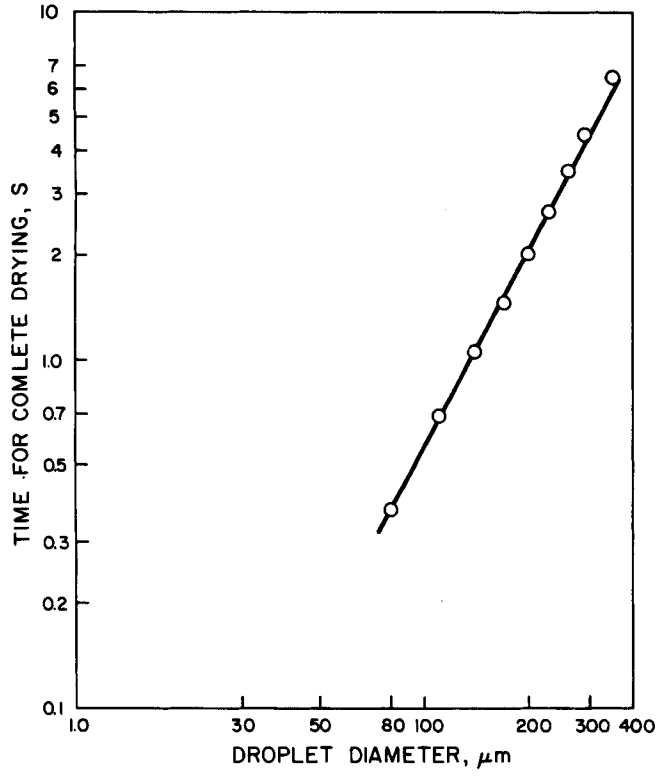

Fig. 12. Drying period as a function of droplet diameter on a log-log plot.

its velocity steadily decreases until it hits the latter.

The axial and radial distances of two droplet sizes as a function of time are given in Figure 10. The large difference in the positions of both droplets, when they are at the desired residual moisture content, illustrates the importance of the largest droplet in the design of spray dryers. The angular position of both 290 and 350 μm droplets as a function of time is shown in Figure 11.

The extent of the drying period, as a function of the droplet diameter, is shown in Figure 12. It is remarkable that a definite monotonic correlation exists between these two variables in spite of the many complexities present in the process. For the particular problem studied here, and for the set of operating conditions chosen, the following correlation can be presented:

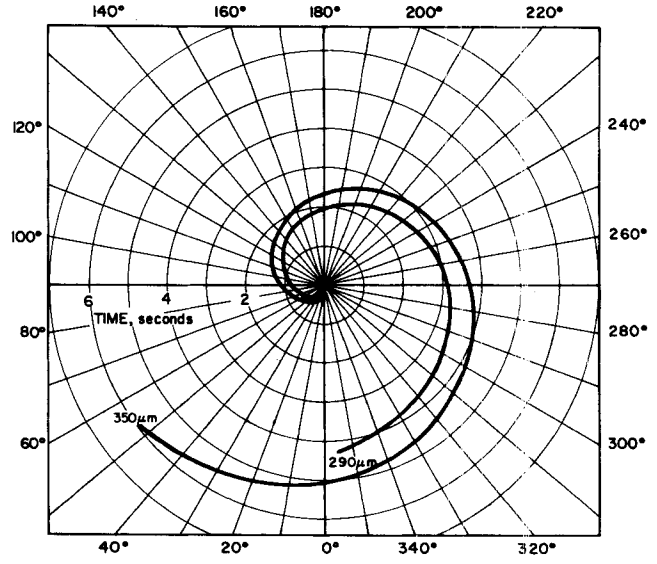

Fig. 11. Angular position of the largest droplet as a function of time.

$$\tau = 1.04 \times 10^{-4} [d_i]^{1.87} \text{ s} \qquad (48)$$

If a correlation can be established between the drying time and the droplet size for any particular process, the design can be carried out merely from a knowledge of the trajectory of the largest droplet. The design procedure can thus be highly simplified.

CONCLUDING REMARKS

The present study has shown that a spray dryer can be designed on a theoretical basis, providing a minimum amount of information is available, which this work has identified as the drying characteristics of the feed solution, the DSD prevailing at or near the atomizing device, and the flow pattern of the drying gas in the chamber. Although the present program is limited to a pressure nozzle, it can be easily modified for other types of atomizers from a knowledge of the entrainment and resulting flow patterns of the gas within the spray. Equations were presented, wherever possible, for other types of atomizers which enable the design of spray dryers in those cases. Indeed, the case of the pneumatic atomizer has already been treated in detail in a previous study (Katta and Gauvin, 1975).

It is hoped that as more experimental evidence becomes available, some of the assumptions which had to be made in the course of the calculations (such as the assumption of negligible radial temperature and humidity gradients in the drying gas) will be removed and refinements in the approach will be effected (such as the choice of a less restrictive design criterion and an estimate of the effects of the turbulence characteristics of the drying medium on the spray drying operation). Concerning the latter, a step in the right direction was taken by Bank (1975) who reported values of the turbulence intensities in the three dimensions in a chamber of similar geometry to the one used here.

Another area which requires attention concerns the drop trajectory calculations in the nozzle zone, since their accuracy is subject to the assumptions which had to be made, owing to lack of information in the literature, regarding the initial spatial distribution of the droplets in the spray and the flow patterns of the gas within the spray. Preliminary estimates of the influence of various alternatives indicate that the effect on the overall design results would, however, be small.

The case of hollow product particles could also be handled by the program but would require a considerable

amount of experimental information on the concentration vs. diameter relationship in the particle during drying. The calculations would become particularly complex if a significant fraction of the hollow particles fragmented during the last stages of the operation.

Finally, it is important to note that the computerized approach proposed here lends itself particularly well to economic evaluations and comparisons between thermal efficiencies, heat requirements, capital and operating costs, etc., arising from changes in design geometry and alternative choices in operating conditions.

ACKNOWLEDGMENT

The authors gratefully acknowledge the financial assistance of the National Research Council of Canada in the form of a special grant.

NOTATION

A_1 = cross-sectional area available for liquid flow at pressure nozzle, cm^2
A = cross-sectional area available for air flow in pneumatic nozzle, cm^2
a, b = parameters in Equations (1) and (6)
b' = parameter defined by Equation (26)
C_1, C_2, C_3, C_4 = constants
C_D = drag coefficient
C_f = heat capacity of feed, J/kg · °K
C_p = heat capacity, J/kg · °K
C_{ps} = heat capacity of solid, J/kg · °K
C_{s1}, C_{s2} = heat capacity of inlet and outlet humid air, J/kg · °K
c = droplet solid concentration, %
d = drop diameter, μm
d_i = diameter of each class of droplets, μm
$\overline{d}$ = mass median drop diameter, μm
d_m = diameter of largest droplet, μm
d_p = characteristic droplet diameter, μm
D_o = diameter of nozzle, cm
d_{vs} = mean Sauter diameter, $\Sigma n_i d_i^3/\Sigma n_i d_i^2$, μm
D_v = diffusivity, cm^2/s
E_x = amount of evaporation up to section x, g/s
E = entrainment parameter, dimensionless
F_L = lift force, N
g = acceleration due to gravity, cm/s^2
G = mass velocity, g/s · (cm of wetted periphery)
h = heat transfer coefficient, $J/m^2 \cdot s \cdot °K$
H = average absolute humidity at any section, g of water vapor/g of dry air
H_1, H_2 = absolute humidities of entering and leaving air, respectively, g of water vapor/g of dry air
H_s = height of spray dryer, cm
H_w = saturation humidity, g of water vapor/g of dry air
k_a = thermal conductivity of air, J/m · s · °K
K = curl of fluid velocity, s^{-1}
k = mass transfer coefficient, g mole/(cm^2 · s)
L_w = wetted periphery of centrifugal-disk atomizer, cm
m = mass of droplet, g
M = molecular weight of air-vapor mixture
M_e = mass flow rate of entrainment, g/s
M_o = mass flow rate of atomizing air, g/s
N = rate of rotation of centrifugal-disk atomizer, rev/s
n = power in Equation (9), −1 or −0.5
n_i = number of each class of droplets
p_1 = liquid pressure at the nozzle, N/cm^2
p_t = pressure in spray-drying chamber, N/cm^2
p_w = vapor pressure at drop surface, N/cm^2
q = rate of heat transfer to droplets, J/s; constant in Equation (6)
q_1 = rate of heat losses from spray chamber, J/s
Q_1 = volumetric flow rate of liquid, m^3/h
Q_a = volumetric flow rate of atomizing air, m^3/h
r = radial position of droplet, cm
r_m = radius of annular region, cm
r_5 = velocity half radius, cm
R_c = radius of cylindrical section, cm
R_d = radius of centrifugal-disk atomizer, cm
R_x = radius of chamber at any height, cm
t = time, s
t_a = temperature of drying air, °K
t_f = feed temperature, °K
t_p = product temperature, °K
t_w = wet bulb temperature of drying air, °K
t_s = droplet temperature, °K
V = volume of feed sample, μm^3
V_{at}, V_{ar}, V_{av} = absolute values of tangential, radial and axial velocities of air, respectively, cm/s
$\overline{V}_{av}$ = average axial velocity of air at any section, cm/s
V_c = velocity of air on the centerline of the spray, cm/s
V_f = resultant velocity of droplet relative to fluid, cm/s
V_f' = cumulative volume fraction less than given size
V_o = average velocity of liquid leaving atomizer and in the case of pneumatic nozzle air velocity at nozzle exit, cm/s
V_t, V_r, V_v = absolute values of tangential, radial and axial velocities of droplet, respectively, cm/s
V_{rel} = relative velocity between the air stream and the liquid stream at the nozzle, m/s
W_A = atomizing air flow rate, g/s
W_g = flow rate of drying air; (free air, measured at 294°K and 1 atm), g of drying air/s
W_1 = flow rate of feed, g/s
W_w = chamber capacity, in g of water evaporated/s
$\overline{x}$ = dimensionless distance, defined by Equation (28)
x = vertical distance from nozzle, cm
x' = length of the liquid sheet, cm

Greek Letters

Γ = gamma function
Δ = increment
Δd = the spread of the droplet size distribution
δ = parameter to express the uniformity of spray, Equation (4)
η = drying thermal efficiency, defined by Equation (47)
θ = half angle of liquid sheet, rad
λ = latent heat of vaporization at t_w, J/kg
μ_a = viscosity of air, N · s/m^2
μ = viscosity of liquid, poises
ν_a = kinematic viscosity of air, m^2/s
ρ_a = density of air, g/cm^3
ρ_f = density of feed, g/cm^3
ρ_α = density of the surroundings of the jet, g/cm^3
ρ = density of droplet, g/cm^3
σ = surface tension of liquid, dynes/cm
τ = drying period, s
ω = angular velocity of droplet, rad/s

Dimensionless Groups

Nu = Nusselt number, hd_i/k_a
Pr = Prandtl number, $c_p\mu_a/k_a$
Re = Reynolds number, $d_iV_f\rho_a/\mu_a$
Sc = Schmidt number, $\mu/D_v\rho_a$
Sh = Sherwood number, $kd_iM/D_v\rho_a$

Subscripts

1 = at the inlet conditions of spray dryer
2 = at the outlet conditions of spray dryer
a = of drying air
$a2$ = of drying air at the exit conditions
d = at datum temperature

i = pertaining to i^{th} class of droplets
in = at initial conditions
o = at nozzle exit
p = of the product
x = at a vertical distance x below the nozzle
w = at wet bulb temperature of the air

LITERATURE CITED

Bailey, G. H., I. W. Slater, and P. Eisenklam, "Dynamic Equations and Solutions for Particles Undergoing Mass Transfer," *Brit. Chem. Eng.*, **15**, 912-916 (1970).

Baltas, L., and W. H. Gauvin, "Transport Characteristics of a Co-Current Spray Dryer," *AIChE J.*, **15**, 772-779 (1969*a*).

———, "Performance Predictions for a Co-Current Spray Dryer," *ibid.*, 764-771 (1969*b*).

———, "Some Observations of Crystallization in Spray Droplets," *Can. J. Chem. Eng.*, **47**, 204-205 (1969*c*).

Bank, Nader, M. Eng. thesis, "Measurements of Flow Characteristics in a Confined Vortex Flow," McGill Univ., Montreal, Canada (1975).

Beard, K. V., and H. R. Pruppacher, "Determination of the Terminal Velocity and Drag of Small Water Drops by Means of a Wind Tunnel," *J. Atm. Sci.*, **26**, 1066 (1969).

Benatt, F. G. S., and P. Eisenklam, "Gaseous Entrainment into Axisymmetric Liquid Sprays," *J. Inst. Fuel*, 309-315 (1969).

Briffa, F. E. J., and N. Dombrowski, "Entrainment of Air into a Liquid Spray," *AIChE J.*, **12**, 708 (1966).

Crowe, C. T., M. P. Sharma, and D. E. Stock, "The Particle—Source-in-Cell (PSI-Cell) Model for Gas-Droplet Flows," publication 75-WA/HT-25, presented at the ASME meeting, Houston, Tex. (Nov. 30-Dec. 4, 1975).

Crowe, C. T., and D. T. Pratt, "Analysis of the Flow Field in Cyclone Separators," *Computers and Fluids*, **2**, 249 (1974).

Domingos, J. J. D., and L. F. C. Roriz, "The Prediction of Trajectories of Evaporating or Burning Droplets," Dept. of Mech. Eng., Instituto Superior Technico, Lisbon, Portugal, RC/30 (1974).

Fabian, J. M., "Particle Trajectories in Free Vortex Flow Fields," Ph.D thesis, Univ. Wash., Seattle (1974).

Friedman, S. J., F. A. Gluckert, and W. R. Marshall, Jr., "Centrifugal Disk Atomization," *Chem. Eng. Progr.*, **48**, 181 (1952).

Gauvin, W. H., S. Katta, and F. H. Knelman, "Drop Trajectory Predictions and Their Importance in the Design of Spray Dryers," *Intern. J. Multiphase Flow*, **1**, 793-816 (1975).

Gluckert, F. A., "A Theoretical Correlation of Spray Dryer Performance," *AIChE J.*, 8, 460 (1962).

Janda, F., "Calculation of the Dimension of Disc Spray Dryers with Intensive Circulation of the Drying Medium," *Intern. Chem. Eng.*, **13**, 649-658 (1973).

Katta, S., and W. H. Gauvin, "Some Fundamental Aspects of Spray Drying," *AIChE J.*, **21**, 143-152 (1975).

———, "Behaviour of a Spray in the Near Vicinity of a Pneumatic Atomizer," *Can. J. Chem. Eng.*, **53**, 556-559 (1975).

Kim, K. Y., and W. R. Marshall, Jr., "Drop-Size Distributions from Pneumatic Atomizers," *AIChE J.*, **17**, 575-584 (1971).

Marshall, W. R., Jr., "Atomization and Spray Drying," *Chem. Eng. Progr. Monograph Ser. 2*, **50**, (1954).

Masters, K., *Spray Drying*, Leonard Hill Books, London, England (1972).

Mochida, T., and Y. Kukita, "Spray Drying," *Kagaku Sochi* (1971-73).

Mugele, R. A., and H. D. Evans, "Droplet Size Distribution in Sprays," *Ind. Eng. Chem.*, **43**, 1317 (1951).

Nelson, P. A., and W. F. Stevens, "Size Distribution of Droplets from Centrifugal Spray Nozzles," *AIChE J.*, **7**, 80-86 (1961).

Nukiyama, S., and Y. Tanasawa, "An Experiment on the Atomization of Liquid," *Trans. Soc. Mech. Engrs. (Japan)*, 4, 86, 138 (1938); **5**, 63, 68 (1939); 11-7 and 11-8 (1940).

Paris, J. R., P. N. Ross, Jr., S. P. Dastur, and R. L. Morris, "Modelling of the Air Flow in a coutercurrent Spray-Drying Tower," *Ind. Eng. Chem. Process Design Develop.*, **10**, 157-164 (1971).

Ranz, W. E., and W. R. Marshall, Jr., "Evaporation from Drops, Part I," *Chem. Eng. Progr.*, **48**, 141 (1952).

———, "Evaporation from Drops, Part II," *ibid.*, **48**, 173 (1952).

Rao, C. S., and A. E. Dukler, "The Isokinetic-Momentum Probe. A New Technique for Measurement of Local Voids and Velocities in Flow of Dispersions," *Ind. Eng. Chem. Fundamentals*, **10**, 520-526 (1971).

Rasbash, D. J., and G. W. V. Stark, "Some Aerodynamic Properties of Sprays," *The Chemical Engineer*, A83 (Dec., 1962).

Schowalter, W. R., and H. F. Johnstone, "Characteristics of the Mean Flow Patterns and Structure of Turbulence in Spiral Gas Streams," *AIChE J.*, **6**, 648-655 (1960).

Sen, D. K., "Dynamics of a Spray Tower," Ph.D. thesis, Univ. Wisc., Madison (1973).

York, J. L., and H. E. Stubbs, "Photographic Analysis of Sprays," *Trans. ASME*, **74**, 1157-1162 (1952).

Manuscript received October 9, 1975; revision received April 6 and accepted April 7, 1976.

A Method of Moments for Measuring Diffusivities of Gases in Polymers

A method of moments has been formulated for the determination of the diffusivity of a gas in a polymer from a step response in a continuous permeation chamber. Contributions of system components other than the polymer are easily factored out to determine the contribution of the polymer alone, and this contribution is then analyzed to calculate the diffusivity. The method has been applied to the measurement of the diffusivities of sulfur dioxide in PTFE (Teflon) and fluorosilicone rubber tubes over a wide temperature range.

R. M. FELDER
C-C MA
and
J. K. FERRELL

Department of Chemical Engineering
North Carolina State University
Raleigh, North Carolina 27607

SCOPE

Traditional methods for measuring the diffusivity of a gas in a polymer involve either passage of the gas through a membrane into a closed chamber in which the pressure is monitored or sorption of the gas in a small polymer sample suspended from a spring whose elongation is monitored. In either experiment, a substantial driving

Correspondence concerning this paper should be addressed to R. M. Felder.